Research Article Vol. 4, No. 2 / 15 February 2021 / OSA Continuum 542

Field aberrations in terms of the Q-polynomial basis and its relationship to the Zernike basis

ANDREA GARCÍA-MORENO,* RENÉ RESTREPO, TOMÁS BELENGUER-DÁVILA, AND LUIS M. GONZÁLEZ-FERNÁNDEZ

Departamento de Óptica Espacial, Instituto Nacional de Técina Aeroespacial (INTA), Carretera Ajalvir Km. 4, 28850 Torrejón de Ardoz, Madrid, Spain
*garciamoa@inta.es

Abstract: The aberrations generated at the image plane of an optical system that includes freeform surfaces described through Q-polynomials can be calculated using nodal aberration theory. By analyzing the definition of each Q-polynomial, they can be compared with Zernike polynomials allowing a relationship between the two bases. This relationship is neither simple nor direct, so a fitting must be made. Once established, the contribution to the aberration field map generated by each surface described through the Q-polynomial can be calculated for any surface that is not at the stop of the system. The Q-polynomials are characterized by their orthogonality in the gradient instead of the surface, which represents an opportunity to restrict the changes in the slope in a simple way and facilitate the manufacturing process. The knowledge of the field aberrations generated by each Q-polynomial allows selecting that which of them are necessary to be introduced as variables in the optimization process for an efficient optimization.

1. Introduction

Freeform optics design and fabrication allow the development of smaller and more compact optical systems, preserving or even enhancing their performances [1]. It allows for instance increasing the field of view with respect to equivalent traditional systems [2], decentering surfaces to avoid an obscuration [3] or improving quality of small cameras for cell phones [4], to achieve ultra-short distances for projectors [5] or to improve illumination systems for automotive industry [6]. For the aerospace industry, it represents a remarkable advantage allowing less optical surfaces, less volume and mass with a significant reduction in associated costs in the mission, a goal strongly pursued in recent years, especially with the growth of the CubeSats [7].

Freeform optics consists on the break of rotational symmetry providing higher degrees of freedom for optical design, allowing a high optical quality recovery in highly aberrated systems. The treatment of aberrations in systems using freeform optics requires a different approach than the traditional theory of aberrations. Raised by Shack [8] and developed by Thompson [9,10], the Nodal Aberration Theory (NAT) is based on the Hopkins Wave Aberration Theory [11] and Buchroeder's work [12] on tilted elements in rotational symmetry optical systems, but it was Fuerschbach et al. [13] who expanded the theory to systems with freeform surfaces described in terms of the Zernike basis. NAT provides a mathematical description of the dependence of the optical aberrations on the field evaluated in the image plane. In addition, NAT can also be used during the design process to calculate the freeform deformation in terms of Zernike polynomials that is required to obtain high optical quality at specific field points (nodes) in the image plane [14]. The theory has been used to analyze the field aberrations generated by freeform surfaces in combination with decenter and tilt surfaces [15,16], by off-axis systems [17,18] and even by systems with bi-conic surfaces [19].

As said before, Fuerschbach et al. [13] expanded NAT to optical systems with surfaces described by Zernike basis and it is the most used representation [20], however, there are more available mathematical options to model any surface which can be classified according to its

#410304 https://doi.org/10.1364/OSAC.410304
Journal © 2021 Received 17 Sep 2020; revised 22 Dec 2020; accepted 22 Dec 2020; published 1 Feb 2021

OSA CONTINUUM

orthogonality [21]. We are interested in orthogonal bases due to their properties, specifically in Q-polynomial basis introduced by Forbes [22] in order to represent aspherical and freeform surfaces, with a specific condition of orthogonality to bring the designer closer to the processes of fabrication and metrology [22–24]. Any arbitrary surface $S(r,\theta)$ can be defined in terms of this basis as

$$S(r,\theta) = \frac{cr^2}{1+\sqrt{1-(1+K)c^2r^2}} + \frac{\delta(u,\theta)}{\sigma(r)} = \frac{cr^2}{1+\sqrt{1-(1+K)c^2r^2}} + \frac{1}{\sigma(r)}\left\{u^2(1-u^2)\sum_{n=0}^{N} a_n^0 Q_n^0(u^2) + \sum_{m=1}^{M} u^m \sum_{n=0}^{N}[a_n^m \cos(m\theta) + b_n^m \sin(m\theta)]Q_n^m(u^2)\right\}, \tag{1}$$

where c and K are the curvature and the conic constant of the base surface, r is the radial coordinate, u is the normalized radial coordinate and θ is the angular coordinate. $Q_n^m(u^2)$ are the Q-polynomials and a_n^m and b_n^m are the associated coefficients corresponding to the cosine and sine components respectively. By last, n represents the radial order while m the azimuthal order. Equation (1) shows the addition of two terms, the first one is the base surface considered to be an on-axis conic surface and the second one has two contributions, an aspheric contribution corresponding to $m = 0$ and a freeform contribution (m>0). The second term of Eq. (1) is not defined along the optical axis, instead, it is defined along the direction normal to the base surface. The factor $\sigma(r)$ is the cosine of the angle between the optical axis and the direction of the base surface normal, so it constitutes a projection factor. The Q-polynomials are defined to fulfill that

$$\left\langle |\nabla\delta(u,\theta)|^2 \right\rangle = \left\langle \left(\frac{\partial\delta}{\partial u}\right)^2 + \frac{1}{u^2}\left(\frac{\partial\delta}{\partial\theta}\right)^2 \right\rangle = \sum_{n,m}[(a_n^m)^2 + (b_n^m)^2], \tag{2}$$

which means that they are a base orthogonal in gradient.

Equation (2) represents the main advantage of this set of polynomials, because there is a direct relationship between the change in the local slope of the surface and the coefficients associated to the Q-polynomials, therefore, a constraint can be introduced directly in the optimization process of the optical design to control the surface slopes. It is well known that the cost of manufacture and the difficulty in metrology of an optical surface increase with the deviation from the best-fit base surface. Thus, 2D Forbes basis (Q-polynomials) constitutes a powerful tool to perform a design that takes into account optical quality, cost of manufacture and possible complication of metrology [25]. Takaki et al. [26] showed an optimization constraint that allows searching for a balance between manufacturability and optical performance in the design of optical systems with freeform surfaces described in terms of orthogonal polynomials (Zernike and Q-polynomials), demonstrating the advantage to use them in optical design process. Additionally, Takaki et al. [27] in other work also demonstrated a lower dependence of degeneracy in freeform surface using Q-polynomials instead of Zernike polynomials.

The expressions for Q-polynomials show that the azimuthal order m corresponds to a kind of shape that increases its order with the radial order n, i.e., azimuthal order $m = 0$ corresponds to defocus and spherical deformation for $n = 0$ and, while the order n increases, the higher orders of spherical deformation appear. Azimuthal order $m = 1$ coincides to tilt deformation for $n = 0$ and, for n>0, coma and higher orders of coma emerge. Azimuthal order $m = 2$ is an astigmatism for $n = 0$ and the higher orders of astigmatism show up for n>0. In the same way, azimuthal order $m = 3$ corresponds to trefoil for $n = 0$ and the higher trefoil orders appear for n>0 and azimuthal order $m = 4$ is a tetrafoil for $n = 0$ and the higher tetrafoil orders emerge for n>0. These polynomials are mathematically and graphically represented by Forbes in [22].

Q-polynomials are very similar to Zernike polynomials but there are some differences between the two basis [28]. The first difference between them is that there are no piston and defocus individual polynomials in the base of Q-polynomials. But, the main difference, as mentioned

OSA CONTINUUM

before, is the direction in which each base is defined, i.e., Zernike polynomials are defined along the optical axis, typically the z-axis, while Q-polynomials are defined along the direction normal to the base surface in each point on the surface. This is the reason why $S(r,\theta)$ expressed by Q-polynomials needs the projection factor $\sigma(r)$. For a base conic surface, in first approximation, the projection factor is

$$\frac{1}{\sigma(r)} = \frac{\sqrt{1-Kc^2r^2}}{\sqrt{1-(1+K)c^2r^2}} = \frac{\sqrt{1-Kc^2r_{max}^2u^2}}{\sqrt{1-(1+K)c^2r_{max}^2u^2}} = \frac{\sqrt{1-KAu^2}}{\sqrt{1-(1+K)Au^2}}. \tag{3}$$

The projection factor from Eq. (3) changes for each radial position on the surface and depends on the parameter $A = c^2r_{max}^2$ and the conic constant K, which implies a dependence on the specific surface.

Summarizing, NAT is usually used to described aberration fields in systems which surfaces are described in terms of the Zernike polynomials basis taking advantage of the description introduced by Fuerschbach et al. [13], however, when a freeform surface is described in using of Zernike polynomials, the local changes on the slope cannot be easily constrained. [26]. Therefore, it would be useful to extend the theory to systems containing freeform surfaces expressed in terms of the Q-polynomials basis, which allows a direct constraint in the local changes of the surface slopes. In this paper, we present a novel and practical way to apply NAT to a system with freeform surfaces described by Q-polynomials and obtain the resulting field aberrations generated by each of them. This is done by previous established relationship between Q-polynomials and Zernike polynomials via fitting. Both basis at same time allow knowing the evolution of optical parameters usually described by Zernike polynomials and using the Q-polynomials, the design can be performed while constraining the deviation of slopes of the surfaces that compose the optical system, therefore, the transformation among basis contributes for optical designers having another useful tool. As far as we know, nobody has developed the transformation in explicit form.

2. From Q-polynomials to Zernike polynomials

Q-polynomials are defined along the normal direction to the base surface which is not constant over the whole surface, except in the case of zero curvature. Therefore, there is not an direct conversion to Zernikes so a fitting must be performed, except in the case of a plane base surface.

To fit each Q-polynomial to Zernike basis, the first step is the approximation perform to the case of a plane base surface. Once the Q-polynomial is described as the sum of the first Zernike polynomial and the residual of the approximation, this residual is analyzed to determine the next Zernike polynomials to be introduced in the fitting. Taking the polynomial $Q_0^2(u^2)$ with radial order $n = 0$ and azimuthal order $m = 2$ as an example, which projection to the optical axis is

$$\frac{\sqrt{1-KAu^2}}{\sqrt{1-(1+K)Au^2}}u^2Q_0^2(u^2)\begin{pmatrix}a_0^2 & b_0^2\end{pmatrix}\begin{pmatrix}\cos 2\theta\\ \sin 2\theta\end{pmatrix} = \frac{\sqrt{1-KAu^2}}{\sqrt{1-(1+K)Au^2}}\frac{1}{\sqrt{2}}\begin{pmatrix}a_0^2 & b_0^2\end{pmatrix}\begin{pmatrix}u^2\cos 2\theta\\ u^2\sin 2\theta\end{pmatrix}, \tag{4}$$

the approximation of this polynomial begins with the astigmatism Zernike polynomial in Fringe ordering (Z_5 and Z_6), with the cosine component and a_0^2 weight associated to Z_5 and the sine component and b_0^2 weight associated to Z_6. Only the results for the cosine component are shown (Fig. 1, Fig. 2 and Fig. 3), the sine component has the same behavior. At the moment, the value of A is kept constant and the fittings are analyzed for different values of the conic constant K. The cases considered are $K = 0$ (sphere), $K = -0.5$ (ellipse), $K = -1$ (parabola) and $K = -1.5$ (hyperbola). The first approximations residuals are shown in Fig. 1(a-d) for the different values of K, note that they exhibit the secondary astigmatism behavior in Zernike polynomial representation Z_{12}. Introducing them in the fit, a shape like the next order of astigmatism Zernike polynomial (Z_{21}) emerge and the resultant residuals are shown in Fig. 1(e-h). Again, that polynomial is

OSA CONTINUUM

introduced in the fit and the corresponding residuals look like the next order of astigmatism (Fig. 1(i-l)) and so on. Thus, this Q-polynomial can be rewritten as a series of Zernike polynomials starting by astigmatism contribution Z_5 plus the higher orders of this Zernike polynomial and the residual continues decreasing by adding more orders. This result does not depend on the conic constant of the base surface, therefore, for different values of K, the same polynomials are involved in the series but different values of the fitted coefficients are required.

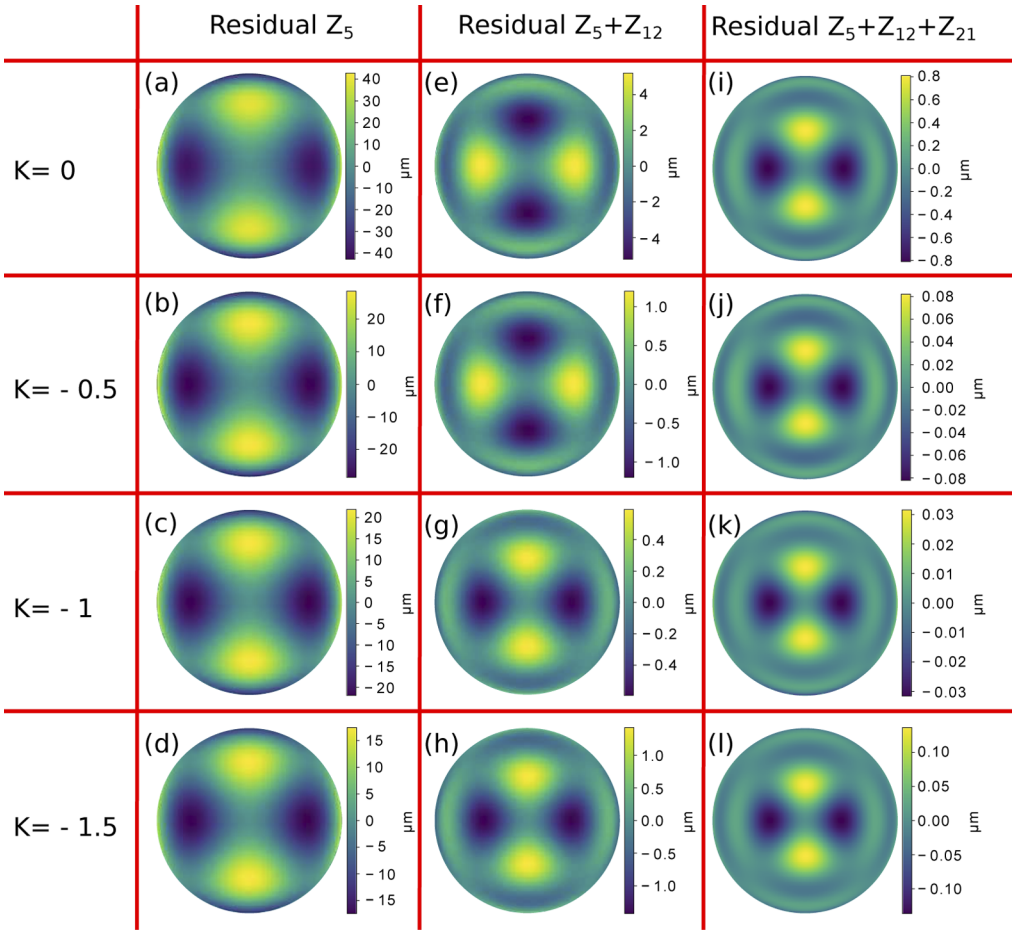

Fig. 1. Example of fit cases. The rows show fits for different K-values (0, −0.5, −1, −1.5). First column maps shows residuals (a to d) from fitting to Z_5, second column maps shows residuals (e to h) from fitting to $Z_5 + Z_{12}$, and finally third column maps shows residuals (i to l) from fitting to $Z_5 + Z_{12} + Z_{21}$. It can be observed how residuals invite to include a higher order of the same type in the next iteration.

In addition, increasing radial order n changes the corresponding Zernike polynomials needed for the first approximation to a plane base surface. That means, having at least $n + 1$ astigmatism polynomials as the first step of the fitting process. The polynomial $Q_1^2(u^2)$ must include at least the sum of Z_5 and Z_{12} for the cosine component in the case of considering a plane base. In the same way, $Q_2^2(u^2)$ must have at least the sum of Z_5, Z_{12} and Z_{21} for the cosine component for a plane base.

OSA CONTINUUM

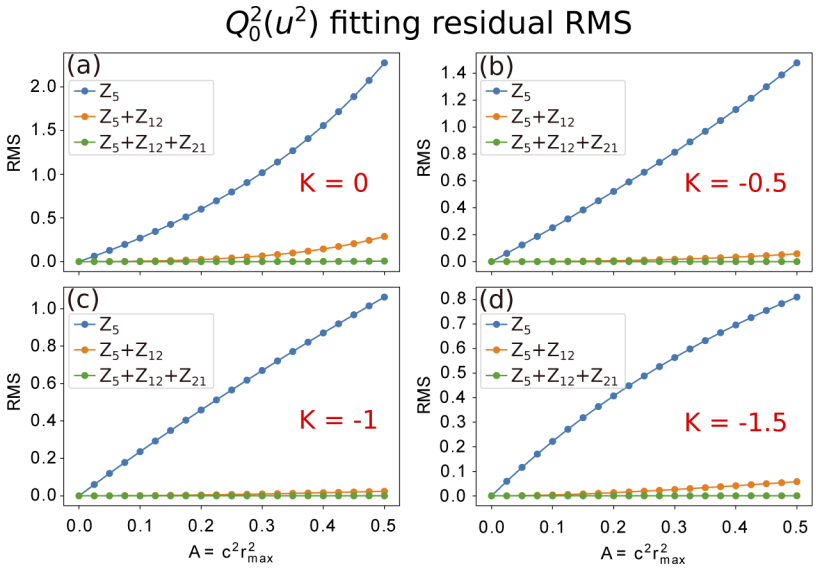

Fig. 2. Residual RMS of fitting $Q_0^2(u^2)$ to 1, 2 and 3 Zernike polynomials in case of (a) $K = 0$, (b) $K = -0.5$, (c) $K = -1$ and (d) $K = -1.5$ in terms of the A parameter. Note that for $A \leq 0.25$, it is possible to achieve an acceptable fitting with few polynomials.

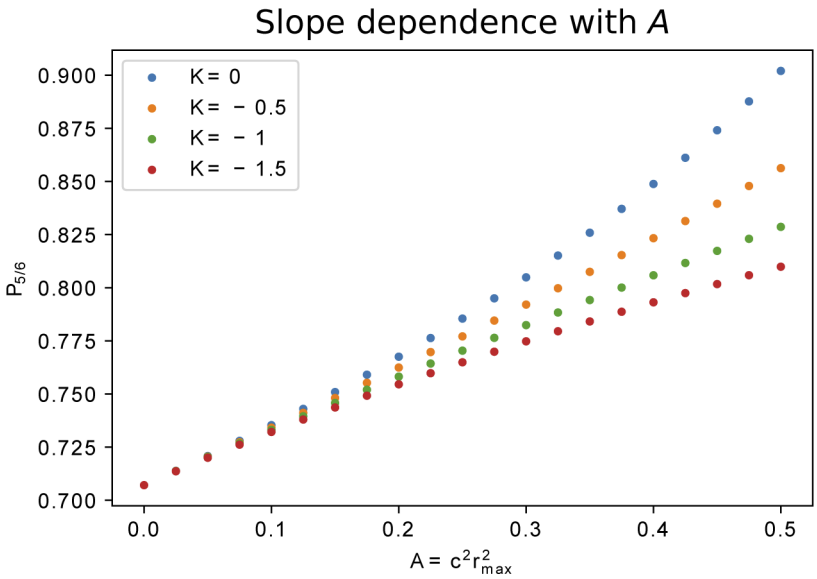

Fig. 3. Slope dependence with A for different conic constants. It can be observed how for A<0.1 the dependence of slope on the value of K is negligible.

OSA CONTINUUM

All these results for the Q-polynomials of order $m = 2$ are mathematically summarized as

$$\begin{aligned}&\frac{\sqrt{1-KAu^2}}{\sqrt{1-(1+K)Au^2}}\frac{1}{\sqrt{2}}\begin{pmatrix}a_0^2 & b_0^2\end{pmatrix}\begin{pmatrix}u^2\cos 2\theta\\ u^2\sin 2\theta\end{pmatrix}\\ &=\begin{pmatrix}C_5 & C_6\end{pmatrix}\begin{pmatrix}Z_5(u,\theta)\\ Z_6(u,\theta)\end{pmatrix}+\begin{pmatrix}C_{12} & C_{13}\end{pmatrix}\begin{pmatrix}Z_{12}(u,\theta)\\ Z_{13}(u,\theta)\end{pmatrix}+\begin{pmatrix}C_{21} & C_{22}\end{pmatrix}\begin{pmatrix}Z_{21}(u,\theta)\\ Z_{22}(u,\theta)\end{pmatrix}+\cdots.\end{aligned} \tag{5}$$

The number of Zernike polynomials required for an acceptable fit depends on the value of the parameter $A = c^2 r_{max}^2$. This parameter can be consider like a shape factor associated with the relationship between the aperture and the radius of curvature of the optical surface and it can only take values between 0 and 1: A is zero for a flat surface and increases towards 1 as the surface becomes more curved and/or larger. Figure 2 shows the root-mean-square (RMS) of the residual obtained after the fitting for the cosine component of $Q_0^2(u^2)$ in terms of A, for a different number of Zernike polynomials considered in the series and for the different values of K. As the value of A gets higher, the surface is further from a plane and higher orders of Zernike polynomials are required. This result does not depend on the value of the conic constant either. However, the residual RMS does depend on K, therefore, the fitting of the polynomial $Q_0^2(u^2)$ might require a different value of polynomials depending of the value of K. For example, for $A = 0.35$, if the base surface is a sphere, the adjustment requires three Zernike polynomials while, if the base surface is a parabola, two are enough.

These results can be generalized for any value of m establishing the relationship between the polynomials in both basis. Consequently, any surface $S(r,\theta)$ expressed by Q-polynomials can be fitted to the corresponding Zernike polynomials in the case of a plane base plus its higher orders. Again, the number of Zernike polynomials needed for the fitting depends on the value of A and K.

A relationship between coefficients can also be calculated and there is a linear dependence between a_0^2 and C_5 and, analogously, between b_0^2 and C_6. The coefficient of determination in the linear fitting always fulfill $R^2 \geq 0.99$ for each relationship between Q-Zernike coefficients in every case of K. The value of the slope obtained by mentioned linear fitting is the same for both components, as a consequence, the relationship between those coefficients can be expressed by $C_5 = P_{5/6}a_0^2$ and $C_6 = P_{5/6}b_0^2$. Note that the R^2 value means a linear dependence that does not change with K, only the magnitude of the slope does.

The linear relationship appears for all values of A, but the value of the slope changes. Figure 3 shows an example of slope $P_{5/6}$ dependence with regard to A parameter using different values of K. Therefore, the slope depends on A and K and must be calculated for each specific surface.

The relationship between Zernike coefficients (C_i) and Q-coefficients (a_n^m, b_n^m) can be generalized. For $m = 0$, $C_i = P_i a_0$ and for $m>0$, $(C_i \quad C_{i+1})^T = P_{i/i+1}(a_0^m \quad b_0^m)^T$, where T means transpose.

3. Aberration fields generated by the Q-polynomials

Nodal Aberration Theory establishes that a freeform surface placed on a position coincident with the aperture stop of an optical system generates aberrations that do not depend on the field. However, while that freeform surface is moved longitudinally away from the stop, the aberrations generated produce a field dependence that is a consequence of the beam displacement on the surface for off-axis fields. For small fields of view the footprint for different fields are approximately circular and identical. Under these conditions the displacement has a linear dependence with the field being defined by $\Delta\vec{h} \equiv (\bar{y}/y)\vec{H} = (\bar{u}t/y)\vec{H}$, where $\bar{y}$ is the chief ray height on the surface, y is the marginal ray height on the surface, $\bar{u}$ is the chief ray angle, t is the distance between the surface and the stop of the system and $\vec{H}$ is the normalized field vector [13].

OSA CONTINUUM

If the surface is described in terms of Zernike polynomials, the expression for the resulting wavefront error by this surface at the stop of the system is given by $W = ((n_2 - n_1)\lambda^{-1}) \sum_i C_i Z_i(u, \theta)$ [16], therefore, the expression for the wavefront error when the surface is at the stop can be rewritten in terms of Q-polynomials using their fitting to Zernike polynomials and the relationships between coefficients. The field aberrations generated while the surface is longitudinally displaced from the stop in terms of Q-polynomials are obtained by introducing the pupil shift $\vec{u} \rightarrow \vec{u} + \Delta\vec{h}$ that is produced by the beam displacement [13].

Notice that freeform surfaces do not introduce any new kind of aberrations but they cause a redistribution of the aberrations with the field. The result is the appearance of nodes of aberrations that are displaced from the optical axis [10,12,13].

Since we are working with Q-polynomials, the notation for the pupil coordinates followed in this paper is that introduced by Forbes [22–24]. Let be $\vec{u}$ the normalized pupil vector, u the normalized radial component and θ the polar component. It differs from the notation adopted in the description of NAT where, $\vec{\rho}$ is the normalized pupil vector, ρ the normalized radial component and ϕ the polar component.

To calculate the field aberrations introduced by each Q-polynomial that defines $S(r, \theta)$, we start from the approximation to a series of Zernike polynomials. As established by the results from Section 2., the number of Zernike polynomials required for the fitting depends on the value of A and K and those values are specific for each base surface. Without lost of generality, we use small value for A parameter with the purpose of using few terms of Zernike polynomials. Additionally, we maintain the value of $n = 0$ while considering different values of m.

Taking the polynomial $Q_0^2(u)$ with radial order $n = 0$ and azimuthal order $m = 2$ as an example, it can be approximated to

$$\frac{\sqrt{1 - KAu^2}}{\sqrt{1 - (1 + K)Au^2}} u^2 Q_0^2(u) \begin{pmatrix} a_0^2 & b_0^2 \end{pmatrix} \begin{pmatrix} \cos 2\theta \\ \sin 2\theta \end{pmatrix} \simeq \begin{pmatrix} C_5 & C_6 \end{pmatrix} \begin{pmatrix} Z_5(u, \theta) \\ Z_6(u, \theta) \end{pmatrix} + \begin{pmatrix} C_{12} & C_{13} \end{pmatrix} \begin{pmatrix} Z_{12}(u, \theta) \\ Z_{13}(u, \theta) \end{pmatrix}. \quad (6)$$

Aberrations when the surface described by the Zernike polynomials is located at the stop are

$$W_{Stop} = \frac{1}{2} \left({}_{FF}\vec{B}_{222}^2 \cdot \vec{u^2} \right) + \frac{1}{2} \left({}_{FF}\vec{B}_{242}^2 \cdot \vec{u^2} \right) (\vec{u} \cdot \vec{u}) - \frac{2}{3} \left({}_{FF}\vec{B}_{242}^2 \cdot \vec{u^2} \right). \quad (7)$$

Equation (7) is described in terms of the Zernike coefficients through the vectors ${}_{FF}\vec{B}_{222}^2 = -2|C_{5/6}|e^{i2\xi_{5/6}}$ and ${}_{FF}\vec{B}_{242}^2 = -8|C_{12/13}|e^{i2\xi_{12/13}}$ that can be expressed in terms of the coefficients associated to polynomial $Q_0^2(u^2)$ through the relations

$$\begin{pmatrix} C_5 \\ C_6 \end{pmatrix} = P_{5/6} \begin{pmatrix} a_0^2 \\ b_0^2 \end{pmatrix}, \qquad \begin{pmatrix} C_{12} \\ C_{13} \end{pmatrix} = P_{12/13} \begin{pmatrix} a_0^2 \\ b_0^2 \end{pmatrix}. \quad (8)$$

Final expressions for ${}_{FF}\vec{B}_{222}^2$ and ${}_{FF}\vec{B}_{242}^2$ in terms of a_0^2 and b_0^2 are summarized as

$${}_{FF}\vec{B}_{222}^2 = -2|C_{5/6}|e^{i2\xi_{5/6}} \equiv 2P_{5/6}\vec{C}_0^2, \quad (9)$$

$${}_{FF}\vec{B}_{242}^2 = -8|C_{12/13}|e^{i2\xi_{12/13}} \equiv 8P_{12/13}\vec{C}_0^2. \quad (10)$$

The vector $\vec{C}_0^2 = C_0^2 e^{i2\xi_0^2}$ represents the magnitude and orientation of polynomial $Q_0^2(u^2)$ and is related to Zernike coefficients by

$$|C_{5/6}| \equiv P_{5/6}C_0^2, \qquad |C_{12/13}| \equiv P_{12/13}C_0^2, \quad (11)$$

$$\xi_{5/6} = \xi_{12/13} \equiv \xi_0^2. \quad (12)$$

OSA CONTINUUM

Thus, the aberrations generated by the surface at the stop of the system in terms of coefficients associated to $Q_0^2(u^2)$ are

$$W_{Stop} = 4P_{12/13}\left(\vec{C}_0^2\cdot\vec{u^2}\right)(\vec{u}\cdot\vec{u}) + \left(P_{5/6} - \frac{16}{3}P_{12/13}\right)\vec{C}_0^2\cdot\vec{u^2}. \tag{13}$$

From Eq. (13) and using NAT as Fuerschbach et al. [13], the aberrations generated when the surface is moved axially away from the stop and their dependence with the field at the image plane can be calculated, introducing the pupil change $\vec{u} \to \vec{u} + \Delta\vec{h}$, as

$$\begin{aligned} W_{NonStop} &= 4P_{12/13}\left(\vec{C}_0^2\cdot\vec{u^2}\right)(\vec{u}\cdot\vec{u}) \\ &+4P_{12/13}\vec{C}_0^2\Delta\vec{h}\cdot\vec{u^3} + 12P_{12/13}\left(\vec{C}_0^2\Delta\vec{h}^*\cdot\vec{u}\right)(\vec{u}\cdot\vec{u}) \\ &+\left[12P_{12/13}\left(\Delta\vec{h}\cdot\Delta\vec{h}\right) + P_{5/6} - \tfrac{16}{3}P_{12/13}\right]\left(\vec{C}_0^2\cdot\vec{u^2}\right) + 12P_{12/13}\left(\vec{C}_0^2\cdot\Delta\vec{h}^2\right)(\vec{u}\cdot\vec{u}) \\ &+\left[8P_{12/13}\left(\Delta\vec{h}\cdot\Delta\vec{h}\right) + 2P_{5/6} - \tfrac{32}{3}P_{12/13}\right]\left(\vec{C}_0^2\Delta\vec{h}^*\cdot\vec{u}\right) + 8P_{12/13}\left(\vec{C}_0^2\cdot\Delta\vec{h}^2\right)\left(\Delta\vec{h}\cdot\vec{u}\right) \\ &+\left[4P_{12/13}\left(\Delta\vec{h}\cdot\Delta\vec{h}\right) + P_{5/6} - \tfrac{16}{3}P_{12/13}\right]\left(\vec{C}_0^2\cdot\Delta\vec{h}^2\right). \end{aligned} \tag{14}$$

In order of appearance, the aberrations shown in Eq. (14) affecting image quality are secondary astigmatism, trefoil, coma, astigmatism and field curvature.

The analysis for the polynomial $Q_0^2(u)$ can also be performed for any other Q-polynomial to obtain the field aberrations. In the Table 1, we summarize the field aberrations for the orders $n = 0$ and $m = 0, 1, 2, 3$. In the first column of the table we show the Q-polynomial and the Zernike coefficients introduced for each fitting (for shortness purposes, piston and tilt are not included).

Table 1. Field aberrations affecting image quality generated by a surface described in terms of each Q-polynomial that is placed away from the stop of the system. The first column shows the Q-polynomial and the Zernike coefficients used for the approximation to obtain $W_{NonStop}$.

	$W_{NonStop}$
$Q_0(u^2)$ (C_1, C_4, C_9, C_{16})	$2a_0\Big\{10P_{16}(\vec{u}\cdot\vec{u})^3 + 60P_{16}\left(\Delta\vec{h}\cdot\vec{u}\right)(\vec{u}\cdot\vec{u})^2 + 60P_{16}\left(\Delta\vec{h}^2\cdot\vec{u^2}\right)(\vec{u}\cdot\vec{u})$ $+20P_{16}\Delta\vec{h}^3\cdot\vec{u^3} + \left[90P_{16}\left(\Delta\vec{h}\cdot\Delta\vec{h}\right) + 3P_9 - 15P_{16}\right](\vec{u}\cdot\vec{u})^2$ $+\left[180P_{16}\left(\Delta\vec{h}\cdot\Delta\vec{h}\right) + 12P_9 - 60P_{16}\right]\left(\Delta\vec{h}\cdot\vec{u}\right)(\vec{u}\cdot\vec{u})$ $+\left[60P_{16}\left(\Delta\vec{h}\cdot\Delta\vec{h}\right) + 6P_9 - 30P_{16}\right]\left(\Delta\vec{h}^2\cdot\vec{u^2}\right)$ $+\left[90P_{16}\left(\Delta\vec{h}\cdot\Delta\vec{h}\right)^2 + (12P_9 - 60P_{16})\left(\Delta\vec{h}\cdot\Delta\vec{h}\right) + P_4 - 3P_9 + 6P_{16}\right](\vec{u}\cdot\vec{u})\Big\}$
$Q_0^1(u^2)$ $(C_2, C_3, C_7, C_8,$ $C_{14}, C_{15})$	$10P_{14/15}\left(\vec{C}_0^1\cdot\vec{u}\right)(\vec{u}\cdot\vec{u})^2 + 30P_{14/15}\left(\vec{C}_0^1\cdot\Delta\vec{h}\right)(\vec{u}\cdot\vec{u})^2$ $+20P_{14/15}\left(\vec{C}_0^1\Delta\vec{h}\cdot\vec{u^2}\right)(\vec{u}\cdot\vec{u}) + 10P_{14/15}\vec{C}_0^1\Delta\vec{h}^2\cdot\vec{u^3}$ $+\left[10P_{14/15}\left[6\left(\vec{C}_0^1\cdot\Delta\vec{h}\right)\Delta\vec{h} + 3(\Delta\vec{h}\cdot\Delta\vec{h})\vec{C}_0^1\right] + (3P_{7/8} - 12P_{14/15})\vec{C}_0^1\right]\cdot\vec{u}(\vec{u}\cdot\vec{u})$ $+\left[10P_{14/15}\left[2\left(\vec{C}_0^1\cdot\Delta\vec{h}\right)\Delta\vec{h}^2 + (\Delta\vec{h}\cdot\Delta\vec{h})\vec{C}_0^1\cdot\Delta\vec{h}\right] + (3P_{7/8} - 12P_{14/15})\vec{C}_0^1\Delta\vec{h}\right]\cdot\vec{u^2}$ $+\left[60P_{14/15}(\Delta\vec{h}\cdot\Delta\vec{h})\left(\vec{C}_0^1\cdot\Delta\vec{h}\right) + (6P_{7/8} - 24P_{14/15})\left(\vec{C}_0^1\cdot\Delta\vec{h}\right)\right](\vec{u}\cdot\vec{u})$
$Q_0^2(u^2)$ $(C_5, C_6, C_{12}, C_{13})$	$4P_{12/13}\left(\vec{C}_0^2\cdot\vec{u^2}\right)(\vec{u}\cdot\vec{u}) + 4P_{12/13}\vec{C}_0^2\Delta\vec{h}\cdot\vec{u^3} + 12P_{12/13}\left(\vec{C}_0^2\Delta\vec{h}^*\cdot\vec{u}\right)(\vec{u}\cdot\vec{u})$ $+\left[12P_{12/13}\left(\Delta\vec{h}\cdot\Delta\vec{h}\right) + P_{5/6} - \tfrac{16}{3}P_{12/13}\right]\left(\vec{C}_0^2\cdot\vec{u^2}\right) + 12P_{12/13}\left(\vec{C}_0^2\cdot\Delta\vec{h}^2\right)(\vec{u}\cdot\vec{u})$
$Q_0^3(u^2)$ $(C_{10}, C_{11}, C_{19}, C_{20})$	$\frac{1}{5}P_{19/20}\left(\vec{C}_0^3\cdot\vec{u^3}\right)(\vec{u}\cdot\vec{u}) + \frac{1}{5}P_{19/20}\vec{C}_0^3\Delta\vec{h}\cdot\vec{u^4} + \frac{4}{5}P_{19/20}\left(\vec{C}_0^3\Delta\vec{h}^*\cdot\vec{u^2}\right)(\vec{u}\cdot\vec{u})$ $+\left[\frac{4}{5}P_{19/20}\left(\Delta\vec{h}\cdot\Delta\vec{h}\right) + P_{10/11} - 4P_{19/20}\right]\left(\vec{C}_0^3\cdot\vec{u^3}\right) + \frac{6}{5}P_{19/20}\left(\vec{C}_0^3\Delta\vec{h}^{*2}\cdot\vec{u}\right)(\vec{u}\cdot\vec{u})$ $+\left[\frac{6}{5}P_{19/20}\left(\Delta\vec{h}\cdot\Delta\vec{h}\right) + 3P_{10/11} - 12P_{19/20}\right]\left(\vec{C}_0^3\Delta\vec{h}^*\cdot\vec{u^2}\right) + \frac{4}{5}P_{19/20}\left(\vec{C}_0^3\cdot\Delta\vec{h}^3\right)(\vec{u}\cdot\vec{u})$

OSA CONTINUUM

4. Design example

To illustrate the results from previous sections, we include the design of a freeform telescope for a spectroscopy application to be used in an Earth observation mission. It is a two-mirror Cassegrain telescope to be embarked on board a CubeSat, therefore, its size is strongly restricted, the entrance aperture and overall length are constraint to a maximum of 80*mm*. None of the mirrors are coincident with the stop of the system as shown in Fig. 4(a). System requirements establish two off-axis regions of 50 microns of diameter located symmetrically along the optical axis where the optical quality must be optimized. These two fields are +/−1.4° off-axis. We appeal to freeform optics to achieve high optical quality.

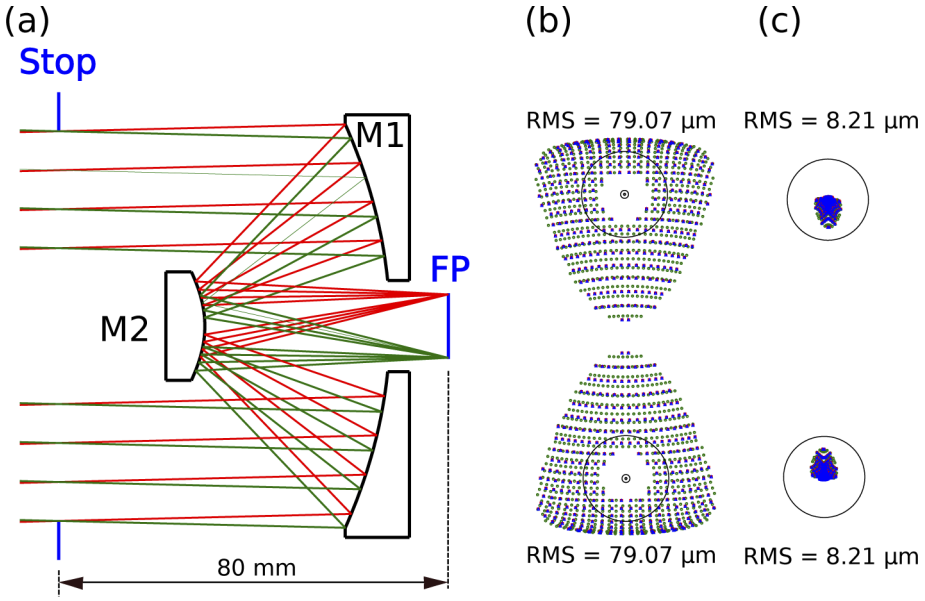

Fig. 4. (a) Freeform telescope layout. Note that the secondary mirror is positioned away from the stop of the system. Spot diagram for the (b) starting symmetric design and the (c) final freeform design. The black circle represents the 50-micron region.

The starting optical design corresponds to the optimized non-freeform solution assuming conic shapes for M_1 and M_2. All the parameters are summarized in Table 2 and the spot diagrams for both fields are shown in Fig. 4(b) where the black circles represent the 50-micron regions.

Table 2. Parameters of the starting non-freeform optimized design.

Surface Name	Surface Type	Y Radius(*mm*)	Conic Constant	Thickness(*mm*)
Stop	Sphere	Infinity	-	68.0
M_1	Conic	−93.4123	−1.0172	−38.0
M_2	Conic	−20.8803	−2.1117	50.0
Image plane	Sphere	Infinity	-	-

Aberrations that limit optical quality are astigmatism and spherical aberration. Therefore, we calculate the Q-polynomials needed to reduce those aberrations for the fields selected, that means, choose the adequate freeform contribution to place the nodes of astigmatism and spherical aberrations at those fields. The primary mirror M_1 remains conic while the secondary mirror M_2 contains the freeform term.

OSA CONTINUUM

The expressions for those aberrations for the starting design (SD) that preserves the rotational symmetry are known and they were described by Hopkins [11] as,

$$W_{ast}^{SD} = \frac{1}{2} W_{222} \vec{H}^2 \cdot \vec{u}^2, \tag{15}$$

$$W_{sph}^{SD} = W_{040} \left(\vec{u} \cdot \vec{u}\right)^2. \tag{16}$$

Due to the field dependence from Eq. (15) and Eq. (16) and the field behavior deduced in Section 3., the Q-polynomials proposed to describe the freeform term to be introduced on the secondary mirror are $Q_0(u^2)$ and $Q_0^2(u^2)$. Note that only the term described by $Q_0^2(u^2)$ is actually a freeform term while $Q_0(u^2)$ describes an aspheric term. The contribution to astigmatism and spherical aberration generated that were calculated in the previous section and correspond to the corresponding terms from Table 1 are

$$\begin{aligned} W_{ast}^{FF} = {} & 2a_0 \left[60P_{16} \left(\vec{\Delta h} \cdot \vec{\Delta h}\right) + 6P_9 - 30P_{16}\right] \left(\vec{\Delta h}^2 \cdot \vec{u}^2\right) \\ & + \left[12P_{12/13} \left(\vec{\Delta h} \cdot \vec{\Delta h}\right) + P_{5/6} - \tfrac{16}{3} P_{12/13}\right] \left(\vec{C}_0^2 \cdot \vec{u}^2\right), \end{aligned} \tag{17}$$

$$W_{sph}^{FF} = 2a_0 \left[90P_{16} \left(\vec{\Delta h} \cdot \vec{\Delta h}\right) + 3P_9 - 15P_{16}\right] \left(\vec{u} \cdot \vec{u}\right)^2. \tag{18}$$

Thus, using the definition of the beam displacement on the surface for off-axis fields $\vec{\Delta h} \equiv (\bar{y}/y)\vec{H}$, the final expressions of the aberrations are

$$\begin{aligned} W_{ast} = {} & \tfrac{1}{2} W_{222} \vec{H}^2 \cdot \vec{u}^2 + 2a_0 \left[60P_{16} \left(\frac{\bar{y}}{y}\right)^2 \left(\vec{H} \cdot \vec{H}\right) + 6P_9 - 30P_{16}\right] \left(\frac{\bar{y}}{y}\right)^2 \left(\vec{H}^2 \cdot \vec{u}^2\right) \\ & + \left[12P_{12/13} \left(\frac{\bar{y}}{y}\right)^2 \left(\vec{H} \cdot \vec{H}\right) + P_{5/6} - \tfrac{16}{3} P_{12/13}\right] \left(\vec{C}_0^2 \cdot \vec{u}^2\right), \end{aligned} \tag{19}$$

$$W_{sph} = W_{040} \left(\vec{u} \cdot \vec{u}\right)^2 + 2a_0 \left[90P_{16} \left(\frac{\bar{y}}{y}\right)^2 \left(\vec{H} \cdot \vec{H}\right) + 3P_9 - 15P_{16}\right] \left(\vec{u} \cdot \vec{u}\right)^2. \tag{20}$$

Then, we need to find the expressions or the coefficients a_0 and $\vec{C}_0^2$ that make zero the Eqs. (19) and (20) for the fields selected. Calling those fields $\vec{H}_1$ and $\vec{H}_2$ and writing all vectors in their exponential form: $\vec{H}_1 = H_1 e^{i\phi_1}$, $\vec{H}_2 = -\vec{H}_1 = H_1 e^{i(\phi_1+\pi)}$, where $\phi_1 = \pi/2$ and $H_1 = 6.5mm$, and $\vec{C}_0^2 = C_0^2 e^{i2\xi_0^2}$, the equations that need to be solved are

$$\begin{aligned} & \left\{ \tfrac{1}{2} W_{222} H_1^2 e^{i2(\phi_1+\alpha)} + 2a_0 \left[60P_{16} \left(\frac{\bar{y}}{y}\right)^2 H_1^2 + 6P_9 - 30P_{16}\right] \left(\frac{\bar{y}}{y}\right)^2 H_1^2 e^{i2(\phi_1+\alpha)} \right. \\ & \left. + \left[12P_{12/13} \left(\frac{\bar{y}}{y}\right)^2 H_1^2 + P_{5/6} - \tfrac{16}{3} P_{12/13}\right] C_0^2 e^{i2\xi_0^2} \right\} \cdot \vec{u}^2 = 0, \end{aligned} \tag{21}$$

$$\left\{ W_{040} + 2a_0 \left[90P_{16} \left(\frac{\bar{y}}{y}\right)^2 H_1^2 + 3P_9 - 15P_{16}\right] \right\} \left(\vec{u} \cdot \vec{u}\right)^2 = 0. \tag{22}$$

In fact, Eq. (21) represents two equations. One first equation for $\alpha = 0$ corresponding to $\vec{H}_1$ and a second one for $\alpha = \pi$ corresponding to $\vec{H}_2$. Starting with Eq. (22), the expression for the coefficient a_0 results to be

$$a_0 = -\frac{1}{2} \frac{W_{040}}{\left[3P_9 - 15P_{16} + 90P_{16} \left(\frac{\bar{y}}{y}\right)^2 H_1^2\right]}. \tag{23}$$

This result only depends on the module of the field H_1, therefore, the position of the node of spherical aberration at the focal plane when the term is introduced and defined by a_0 looks like a ring with radius H_1.

OSA CONTINUUM

In the case of Eq. (21), comparing modules and exponents, the result is

$$\xi_0^2 = \phi_1 + \alpha, \qquad \alpha = 0, \pi, \tag{24}$$

$$C_0^2 = -\frac{\left[\frac{1}{2}W_{222} + 2a_0\left[60P_{16}\left(\frac{\bar{y}}{y}\right)^2 H_1^2 + 6P_9 - 30P_{16}\right]\left(\frac{\bar{y}}{y}\right)^2\right]}{12P_{12/13}\left(\frac{\bar{y}}{y}\right)^2 H_1^2 + P_{5/6} + \frac{16}{3}P_{12/13}}H_1^2. \tag{25}$$

This result shows that introducing a term generated by $\vec{C}_0^2$ produces the appearance of 2 nodes of astigmatism at 2 different positions at the image plane that are symmetric with respect to the axis. Equations (24) and (25) show that the two nodes share the same module but differ in the azimuthal coordinate.

The freeform mirror M_2 has $9.1815mm$ of aperture which means that $A = 0.1934$. With that value of A and the conic constant from Table 2, the vales of the slopes for M_2, calculated as shown in Section 2., are $P_{5/6} = 0.7495$, $P_{12/13} = 0.0126$, $P_9 = -0.1715$ and $P_{16} = -0.0039$. The values of $W_{222} = -0.0187\lambda$ and $W_{040} = 5.0077\lambda$ (at $\lambda = 560nm$) are obtained from the analysis of the starting design in Code V (Synopsys, USA). Thus, the values for a_0 and $\vec{C}_0^2$ can be calculated analytically, where $a_0 = 1.5819\mu m$, $C_0^2 = 4.7006\mu m$ and $\xi_0^2 = \pi/2 + \alpha$ with $\alpha = 0, \pi$. Note that C_0^2 and ξ_0^2 are the module and phase respectively of vector (a_0^2, b_0^2). The values obtained for ξ_0^2 make the value of the sine component b_0^2 to be zero and the value of the cosine component a_0^2 to be the value of the module C_0^2 (nodal axis is in vertical direction). With those values, the full-field displays (FFDs) are calculated analytically for astigmatism and spherical aberrations and shown in Fig. 5(c,d). This figures clearly show the appearance of the two nodes of aberrations in compare to the FFDs obtained by Code V for the starting non-freeform design (Fig. 5(a,b)).

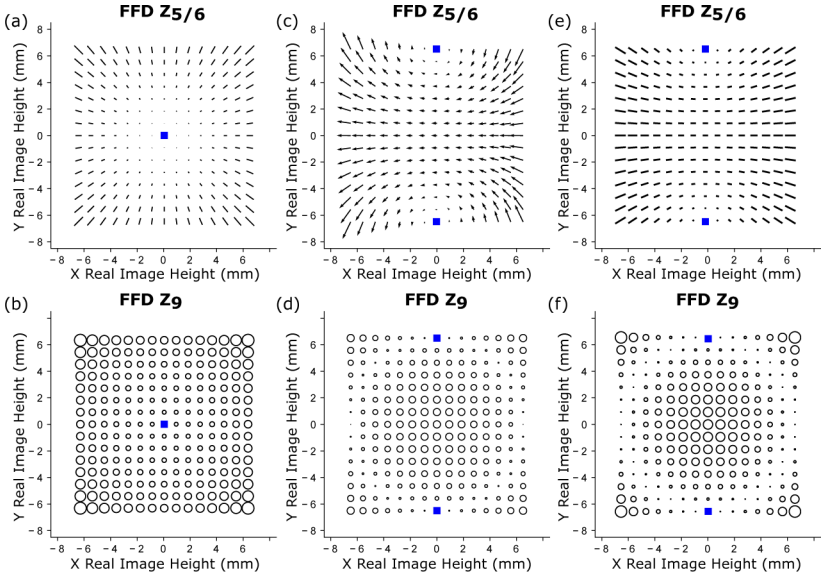

Fig. 5. Full-field maps. (a) Astigmatism and (b) spherical aberration calculated by Code V for the starting non-freeform design. There is only one node of aberration placed at the optical axis. (c) Astigmatism and (d) spherical aberration analytically calculated for the freeform design. The nodes of aberrations appear at the field positions selected. (e) Astigmatism and (f) spherical aberration calculated by Code V for the freeform design. The position of the nodes matches the obtained by the analytical calculations.

OSA CONTINUUM

Identical values for a_0 and $\vec{C}_0^2$ are obtained when the freeform system has been optimized in Code V adapting the merit function to the one used analytically, which minimizes only astigmatism and spherical aberration.

The system has been further optimized in Code V with a merit function containing all the aberrations. In this case, the values for the coefficients are $a_0 = 1.0974\mu m$ and $C_0^2 = 4.6784\mu m$, the spot diagram is shown in Fig. 4(c) and the full-displays obtained are shown in Fig. 5(e,f) for astigmatism and spherical aberration. The differences in the values of a_0 and C_0^2 and the FFDs are associated with merit function used in Code V. The analytical analysis only minimizes astigmatism and spherical aberration according to the fulfillment of the instrument requirements while Code V can minimize more aberrations.

5. Discussion

In this paper, we have performed an analysis of Q-polynomials basis to achieve an efficient transformation to Zernike polynomials. The main difference between the two bases is the axis in which they are defined. In Zernike basis is along the optical axis while in Q-polynomials basis is along the normal to the base surface. This implies that the angle between the two axes changes along the aperture of the surface and the transformation need to be by fitting. However, both axes are coincident in the case of having a plane base surface, so instead of trying to make the fitting using a large number of Zernike terms we start approximating the base surface to a plane. The residual of this fit is approximated again to a Zernike basis and the process repeats itself in a recursive way observing that only similar but higher order Zernike modes appear when the iterations are extended.

This is a very efficient strategy because Zernike polynomials with zero coefficients will never be included in the fitting of the corresponding Q-polynomial. The results show that each Q-polynomials can be expressed as a series of Zernike polynomials. The first term is the corresponding Zernike polynomial in case of having a plane base surface and it is followed by the higher orders of this polynomial. It has been shown that the transformation between basis depends on the parameter A associated to the shape of the base surface. The value of A, which goes from 0 to 1, indicates how strong the curvature of the base surface is with respect to its aperture. It is also related to the angle between the definition axes for each of the basis and determines the number of polynomials needed for the fitting. $A = 0$ means that the base surface is a plane while approaching 1 makes the curvature stronger and requires a greater number of Zernike polynomials to achieve an acceptable fitting. This is a significant information for the designer because it allows to search for a value as close as possible to 0 reducing the complications in the transformation and, consequently, on the use of NAT for a specific design. Furthermore, this property is relevant in typical catoptric systems such as those used for example in aerospace applications where A values are expected to be low (large apertures and moderate curved surfaces). In this case the validity of the fit is demonstrated with a few terms.

The results shown in this document should be seen as an extension of the NAT to optical systems with freeform surfaces described in terms of Q-polynomials and placed far from the stop. They have been achieved by fitting the Q-polynomials to the Zernike polynomials which depends on the value of A which is different for each surface. However, with the results presented, the designer does not need to fit each surface to know which Q-polynomials the system requires. The specific coefficients that must be entered as variables in the optimization process can be obtained only through the field dependence of aberrations as presented in Section 3. It is even possible to obtain an initial value for these coefficients and enter it in the optical design without performing the fit. Fitting is only necessary if the exact value of each coefficient needs to be calculated analytically.

Results show several steps to obtain a freeform design described by Q-polynomials in an effective way. The first step would be the optimization of a starting non-freeform design and the

OSA CONTINUUM

analysis of the main aberrations limiting the optical quality for the specific fields and fulfilling all the constraints for the system. Next, select the adequate Q-polynomials to described the freeform contribution to the system according to the field dependence shown in Table 1. These can be rewritten in terms of Zernike polynomials and the relationship between coefficients can be obtained. The specific values for coefficients associated to Q-polynomials ($\vec{C}_n^m$) that locates the nodes of aberrations at the fields of interest can also be calculated. With these calculations, the system would be optimized and can also be introduced in Code V for a more precise optimization than achieved analytically. Code V also allows to introduce the constraint on the local changes of the slope of the system. To fulfill that constraint might not be enough to introduce the order $n = 0$, higher n-orders with the same value of m may be required. Last, the results from Section 2 provide the option of changing the basis to Zernike polynomials. It is useful to use both basis, each of them in the most adequate context. When designing, using Q-polynomials allows introducing the constraint in the slopes so a manufacturing oriented design can be performed. However, Zernike basis is more appropriate because it is the most extended basis, provides a better understanding of the individual modes and import/export function for other applications.

The proposed method is limited to moderate fields so the shift $\Delta\vec{h}$ can be approximated to have a linear dependence with the field. Also, the so useful orthogonality condition that Q-polynomials exhibit is limited to circular apertures. Last, as the system requires a fitting with higher order Zernike polynomials, the mathematical analysis becomes complex.

As an illustrative example of the results, the design of a 2-mirror Cassegrain telescope with a freeform contribution defined by $Q_0^2(u^2)$ has been shown. Following the procedure described before, the analytical solution has shown to predict the behavior of the main aberrations of the system and the distribution of nodes at the image plane.

6. Conclusions

Q-polynomials basis brings the manufacturing and metrology processes closer to the designer thanks to the orthogonality in the gradient that allows introducing a restriction in the changes of the slope of a surface in a simple way. The adaptation of the Nodal Aberration Theory to freeform systems where surfaces are described in terms of Q-polynomials is an added value that allows calculating the field aberrations generated by these surfaces and the positions of the aberration nodes in the image plane. NAT definition by Q-polynomials made in this work constitutes a manufacturing-oriented tool for the optical designer that allows, as seen in the practical case, to customize the fields of minimum aberration during the optimization process taking advantage of their orthogonality condition.

Disclosures. The authors declare that there are no conflicts of interest related to this article.

References

1. F. Fang, X. Zhang, A. Weckenmann, G. Zhang, and C. Evans, "Manufacturing and measurement of freeform optics," CIRP Ann. **62**(2), 823–846 (2013).
2. Q. Meng, H. Wang, W. Liang, Z. Yan, and B. Wang, "Design of off-axis three-mirror systems with ultrawide field of view based on an expansion process of surface freeform and field of view," Appl. Opt. **58**(3), 609–615 (2019).
3. C. Xu, D. Cheng, and Y. Wang, "Automatic obscuration elimination for off-axis mirror systems," Appl. Opt. **56**(32), 9014–9022 (2017).
4. C. Hou, Y. Ren, Y. Tan, Q. Xin, and Y. Zang, "Ultra slim optical zoom system using Alvarez freeform lenses," IEEE Photonics J. **11**(6), 1–10 (2019).
5. F. Fournier and J. Rolland, "Optimization of freeform lightpipes for light-emitting-diode projectors," Appl. Opt. **47**(7), 957–966 (2008).
6. R. A. Hicks, "Controlling a ray bundle with a free-form reflector," Opt. Lett. **33**(15), 1672–1674 (2008).
7. T. Agócs, R. Navarro, N. Tromp, and R. Vink, "Freeform mirror based optical systems for nano-satellites," in *International Conference on Space Optics—ICSO 2016*, vol. 10562 (International Society for Optics and Photonics, 2017), p. 1056228.
8. R. V. Shack and K. Thompson, "Influence of alignment errors of a telescope system on its aberration field," in *Optical Alignment I*, vol. 251 (International Society for Optics and Photonics, 1980), pp. 146–153.

OSA CONTINUUM

9. K. Thompson, "Description of the third-order optical aberrations of near-circular pupil optical systems without symmetry," J. Opt. Soc. Am. A **22**(7), 1389–1401 (2005).
10. K. P. Thompson, "Aberration fields in tilted and decentered optical systems," Ph.D. thesis, University of Arizona (1980).
11. H. H. Hopkins, *Wave theory of aberrations* (Clarendon Press, 1950).
12. R. A. Buchroeder, "Tilted component optical systems," Ph.D. thesis, University of Arizona (1976).
13. K. Fuerschbach, J. P. Rolland, and K. P. Thompson, "Theory of aberration fields for general optical systems with freeform surfaces," Opt. Express **22**(22), 26585–26606 (2014).
14. E. M. Schiesser, A. Bauer, and J. P. Rolland, "Estimating field-dependent nodal aberration theory coefficients from zernike full-field displays by utilizing eighth-order astigmatism," J. Opt. Soc. Am. A **36**(12), 2115–2128 (2019).
15. H. Shi, H. Jiang, X. Zhang, C. Wang, and T. Liu, "Analysis of nodal aberration properties in off-axis freeform system design," Appl. Opt. **55**(24), 6782–6790 (2016).
16. T. Yang, D. Cheng, and Y. Wang, "Aberration analysis for freeform surface terms overlay on general decentered and tilted optical surfaces," Opt. Express **26**(6), 7751–7770 (2018).
17. G. Ju, C. Yan, Z. Gu, and H. Ma, "Aberration fields of off-axis two-mirror astronomical telescopes induced by lateral misalignments," Opt. Express **24**(21), 24665–24703 (2016).
18. G. Ju, H. Ma, and C. Yan, "Aberration fields of off-axis astronomical telescopes induced by rotational misalignments," Opt. Express **26**(19), 24816–24834 (2018).
19. Y. Zhong and H. Gross, "Vectorial aberrations of biconic surfaces," J. Opt. Soc. Am. A **35**(8), 1385 (2018).
20. T. Yang, J. Zhu, and G. Jin, "Nodal aberration properties of coaxial imaging systems using zernike polynomial surfaces," J. Opt. Soc. Am. A **32**(5), 822–836 (2015).
21. J. Ye, L. Chen, X. Li, Q. Yuan, and Z. Gao, "Review of optical freeform surface representation technique and its application," Opt. Eng. **56**(11), 1 (2017).
22. G. Forbes, "Characterizing the shape of freeform optics," Opt. Express **20**(3), 2483–2499 (2012).
23. G. Forbes, "Robust, efficient computational methods for axially symmetric optical aspheres," Opt. Express **18**(19), 19700–19712 (2010).
24. G. Forbes, "Fitting freeform shapes with orthogonal bases," Opt. Express **21**(16), 19061–19081 (2013).
25. G. Forbes, "Manufacturability estimates for optical aspheres," Opt. Express **19**(10), 9923–9942 (2011).
26. N. Takaki, A. Bauer, and J. P. Rolland, "On-the-fly surface manufacturability constraints for freeform optical design enabled by orthogonal polynomials," Opt. Express **27**(5), 6129–6146 (2019).
27. N. Takaki, A. Bauer, and J. P. Rolland, "Degeneracy in freeform surfaces described with orthogonal polynomials," Appl. Opt. **57**(35), 10348–10354 (2018).
28. I. Kaya, K. P. Thompson, and J. P. Rolland, "Comparative assessment of freeform polynomials as optical surface descriptions," Opt. Express **20**(20), 22683–22691 (2012).